SUBMISSION TO GÈOTECHNIQUE

DATE:
Written 03 October 2017
Revised 18 May 2018

TITLE:
Mechanisms of failure in saturated and unsaturated clayey geomaterials subjected to (total) tensile stress

AUTHORS:
Ian Murray*
Alessandro Tarantino **

POSITION AND AFFILIATION:
* PhD graduate, Department of Civil and Environmental Engineering, University of Strathclyde
** Professor, Department of Civil and Environmental Engineering, University of Strathclyde

CONTACT ADDRESS:
Professor Alessandro Tarantino
Department of Civil and Environmental Engineering
University of Strathclyde
James Weir Building - Level 5
75 Montrose Street - Glasgow G1 1XJ, Scotland, UK
E-mail: alessandro.tarantino@strath.ac.uk

KEYWORDS
Clay, tensile failure, high-capacity tensiometer, plastic limit, cavitation

MECHANISMS OF FAILURE IN SATURATED AND UNSATURATED CLAYEY GEOMATERIALS SUBJECTED TO (TOTAL) TENSILE STRESS

I. MURRAY AND A. TARANTINO

Abstract

The paper presents an experimental investigation into the mechanisms of tensile failure in clayey geomaterials under saturated and unsaturated conditions. An experimental apparatus was developed to test specimens in uniaxial tension with the facility to monitor suction (pore-water tension) using high-capacity tensiometers. This allowed interpretation of failure data in terms of effective stress and average skeleton stress for saturated and unsaturated specimens respectively. Experimental data from normally consolidated samples showed that failure under uniaxial tension occurs in shear and tensile cracks form as a combination of Mode I and Mode II fracture. In the saturated range when samples were prepared with de-aired water, tensile failure occurred at deviatoric stresses corresponding to the critical state line derived from triaxial and uniaxial compression tests. When using non-de-aired water and at suction levels approaching the air-entry value, failure occurred at deviatoric stresses lower than the ones corresponding to the critical state line derived from compression tests. It has been suggested that water cavitation may be one of the mechanisms that control premature rupture of saturated clay when subjected to a (total) tensile stress state. Finally, tensile failure data from unsaturated samples showed that there is continuity between saturated and unsaturated states.

1. INTRODUCTION

Tensile stresses may develop in geotechnical structures due to desiccation-induced shrinkage (e.g. Morris et al. 1992; Konrad and Ayad 1997), decrease in lateral stress (e.g. Hughes et al. 2007), and differential deformations (e.g. Sherard 1986; Handy and Lustig 2017). Tensile stresses may lead to the formation of tension cracks, which can compromise the performance of geotechnical structures due to their effects on soil mechanical and hydraulic behaviour.

The presence of tension cracks influences the stability of natural slopes (Baker 1981) and flood embankments due to water seeping into the desiccated crest (Marsland & Cooling, 1958; Marsland, 1968; Marnette et al. 2006). Tension cracks significantly increase the hydraulic conductivity of clayey soils providing a preferential pathway for fluid transport (Yesiller et al. 2000; Albrecht & Benson, 2001; Greve et al. 2010). Tension cracks are also important in the ceramic industry as they develop in wares during the drying of slip cast forms (Cooper, 1978; Tarantino et al., 2010).

Understanding the mechanisms of failure under tension is key to model tension crack initiation and propagation. Tension cracks are commonly assumed to develop when tensile stresses exceed the soil tensile strength (Morris et al., 1992; Konrad and Ayad, 1997; Rodriguez et al., 2007; Prat et al., 2008; Peron et al., 2009; Amarasiri et al., 2011; Sima et al., 2014; Sanchez et al., 2014). However, the conditions leading to failure under a tensile stress state are still controversial.

Tensile failure criteria have been formulated in terms of a threshold value of the minimum principal stress, implicitly assuming that failure occurs in Mode I fracture. This threshold value has been determined directly via uniaxial tensile tests (e.g. Tang and Graham 2000; Kim and Hwang, 2003; Rodriguez et al., 2007; Lakshmikantha et al. 2012; Trabelsi et al. 2012) or indirectly via Brazilian and bending tests (e.g. Ajaz and Parry, 1975; Thusyanthan

et al. 2007; Villar et al 2009; Stirling et al 2015). The threshold value of the minimum principal stress is generally characterised in terms of total stress and is often referred to as 'tensile strength'. Tensile strength has been observed to depend on soil density (e.g. Trabelsi et al. 2012), moisture content (e.g. Amarasiri et al., 2011; Trabelsi et al. 2012; Stirling et al. 2015), and degree of saturation (e.g. Heibrock et al. 2005; Rodriguez et al. 2007; Trabelsi et al. 2012). To characterise the tensile strength of a soil, authors have generally established empirical relationships between the tensile strength and one of these phase variables (density, water content or degree of saturation), making the implicit assumption that the other remaining variables do not affect tensile strength significantly. The choice of the phase variable controlling the tensile strength then appears to be left to the intuition of the researchers carrying out a specific experimental programme. This makes it difficult to lay down a more general conceptual framework for the failure response of soil subjected to tensile stresses.

At a more fundamental level, the characterisation of soil response in terms of total stress is questionable. Crack initiation in geomaterials prepared from slurry often occurs at the transition from saturated to unsaturated states upon a drying process (Bowman, 1926; Clews, 1969; Peron et al., 2007; Peron et al. 2009). In the saturated state, it would be expected that the response of the clay is modelled in terms of effective and not total stress. Even in the unsaturated range, it would be expected that the response of the soil is controlled by generalised effective stresses, which would include not only the total stress but also the (negative) pore-water pressure and other phase variables, such as the degree of saturation and porosity (Houlsby 1997). Characterising the response of soils in terms of total stress therefore appears to be in contradiction with the concept of effective stress, the pillar around which modern soil mechanics has been built.

Soils under a tensile (total) stress are generally characterised by negative pore-water pressures that are difficult to measure. This is likely the reason why the majority of direct and indirect tensile tests were carried out without the measurement of negative pore-water pressure, with experimental data therefore inevitably interpreted in terms of total stress. The experimental programmes carried out by Avila (2004) and Thusyanthan et al. (2007) appear to be the only examples where negative pore-water pressures were measured in soils subjected to tensile (total) stress. Thusyanthan et al. (2007) showed that failure in saturated soils occurs in shear rather than tension, i.e. tensile failure is controlled by the combination of isotropic and deviatoric effective stresses rather than a threshold value of (negative) minimum principal total stress. They also showed that the formation of a tension crack occurs under a combination of Mode I and Mode II fracture. Avila (2004) also observed that failure in uniaxial tension tests occurs in shear although at a friction angle significantly lower than the friction angle characterising failure in triaxial compression and extension. Shin and Santamarina (2011) also suggested that the formation of tension cracks in saturated geomaterials is controlled by the effective stress.

Thusyanthan et al. (2007) have explored the mechanisms of tensile failure in saturated geomaterials but the question still remains open about the mechanisms of crack initiation in unsaturated geomaterials. Morris et al. (1992), Lakshmikantha et al. (2012), Tang et al. (2015), and Varsei et al. (2016) have implicitly suggested that crack initiation in unsaturated geomaterials can be modelled in terms of 'average skeleton stress' (Tarantino, 2007; Alonso et al. 2010; Tarantino and El Mountassir, 2013) or net stress and suction. However, there is no direct experimental evidence of the validity of such an assumption.

This paper presents an experimental programme with the aim of clarifying fundamental aspects of failure under tension. Tests include a new direct method of tensile testing using

high capacity tensiometers to measure negative pore-water pressure during testing. Samples have been tested in the saturated and unsaturated range. Saturated samples were initially prepared with non-de-aired water and tested in uniaxial tension. A second series of samples was then prepared using de-aired water to probe the hypothesis that early failure might be triggered by the process of water cavitation. A third series of samples were finally tested in the unsaturated range.

2. MATERIALS AND SPECIMEN PREPARATION

Materials used

Two materials were used in the experiments, Speswhite kaolin (SK, silty clay) and a material mix commonly used in the ceramics industry, Vitreous China (VC). The grain size distributions showed them to have 0.25 silt fraction and 0.75 clay fraction for SK and 0.70 silt fraction and 0.30 clay fraction for VC.

Preparation of non-de-aired samples

Specimens were prepared by slip casting in plaster moulds. The suction possessed by the plaster removes water from the liquid slip to create a plastic specimen. The moulds for the uniaxial tensile/compression and triaxial specimens created a specimen of the required shape for testing, whereas the mould for the water retention curve creates a large bar from which specimens were made using a cutting ring.

A large quantity of the VC slip was prepared by mixing the dry powdered constitutive parts with demineralised water and stored in an air tight container for the period of the experiments. Individual specimens were prepared by taking a portion of the slip, which had

been mixed for 30 minutes, and adding de-mineralised water to reach target the gravimetric water content (w≈0.35). The Speswhite kaolin was prepared before each experiment by mixing the kaolin powder with demineralised water to a moisture content of approximately 2.5 (250%).

The time required to consolidate the VC slip in the mould varied in the range of 90-150 minutes depending upon the specimen shape being made. Upon removal from the mould the moisture content of the specimens was in the range of 0.2-0.21, corresponding to an initial pore-water pressure of approximately 100kPa. The time required to consolidate the slip of SK was higher (120-150 min) due to the higher initial water content. Upon removal from the moulds the moisture content was 0.54, corresponding to an initial pore-water pressure of approximately -100kPa.

De-aired samples

The SK and VC slips, prepared to the correct moisture content, were added into a vacuum chamber. The vacuum chamber was placed on top of a stirring plate and a stirring rod added to the slip. A vacuum of ~100kPa was applied to the chamber for a period of one hour. The slip was stirred continuously throughout the de-airing process. At the end of the de-airing process no more bubbles of air were being visibly released from the slip. The slip was then cast immediately in the plaster moulds.

3. EQUIPMENT

High-Capacity Tensiometer

The measurement of matric suction was performed using high capacity tensiometers

(Tarantino & Mongiovi, 2002). The tensiometers are comprised of a water reservoir, a high air entry ceramic disk (1.5MPa) and an integral strain gauge diaphragm.

Chilled Mirror Psychrometer

Measurement of suction beyond the range of the tensiometers was done using a WP4C water potential meter. The WP4C uses the chilled mirror method to determine the relative humidity of the air around a sample in a sealed chamber once the sample has come into equilibrium with the vapour in the surrounding air. Calibration of the device was achieved by using sodium chloride solutions with known relative humidity.

Uniaxial tensile test apparatus

The uniaxial tensile test apparatus was designed to operate in load-control mode with high capacity tensiometers used to measure the matric suction of the specimen throughout testing. The test specimen has a thickness of 15 mm and a centre section with a cross sectional area equal to one third of that at the ends (Figure 1). This results in a higher axial stress within the central area, and failure subsequently occurs in this centre section. The end sections are curved towards the centre section, resulting in a smooth transition between the centre section and curved section.

The specimen is fixed, using a glue, at one end to a rigid restraint and at the opposite end to a rigid plate from which a hanger is attached via a low friction wheel (Figure 2). The specimen is placed on top of a layer of ball bearings to reduce frictional effects and allow the sample to deform during loading. A plastic paraffin film was used to cover the specimen during glue curing and testing to control and reduce as much as was possible evaporation from the specimen. Each test used three tensiometers placed onto the surface of the specimen to measure the suction of the sample. One was secured to each end of the sample and a third

was located in the centre section. The suction measured by the centre tensiometer was used in the test analysis. The tensiometers at the ends were used to check the consistency of the suction measured by the centre tensiometer.

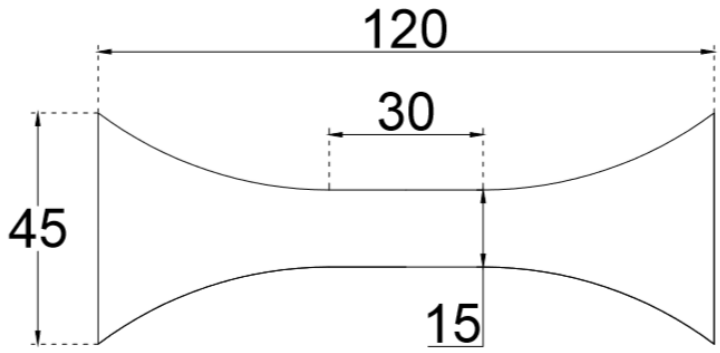

Figure 1 Uniaxial tension and compression specimen shape and dimensions (mm)

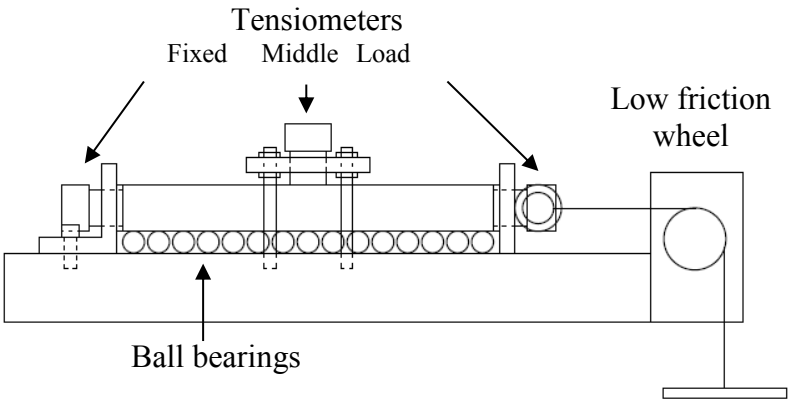

Figure 2 Apparatus for uniaxial tension test

Uniaxial compression test apparatus

Uniaxial compression testes were carried out on specimens having same dimensions as tensile tests. To impose a compressive load, the tensile test apparatus was mounted for convenience

inside the tensile test apparatus of Rodriguez (2002) as shown in Figure 3. Tensiometers were only located at the ends of the specimen. A tensiometer in the centre section was tried but it was not possible to maintain a good connection between the tensiometer and the specimen throughout loading.

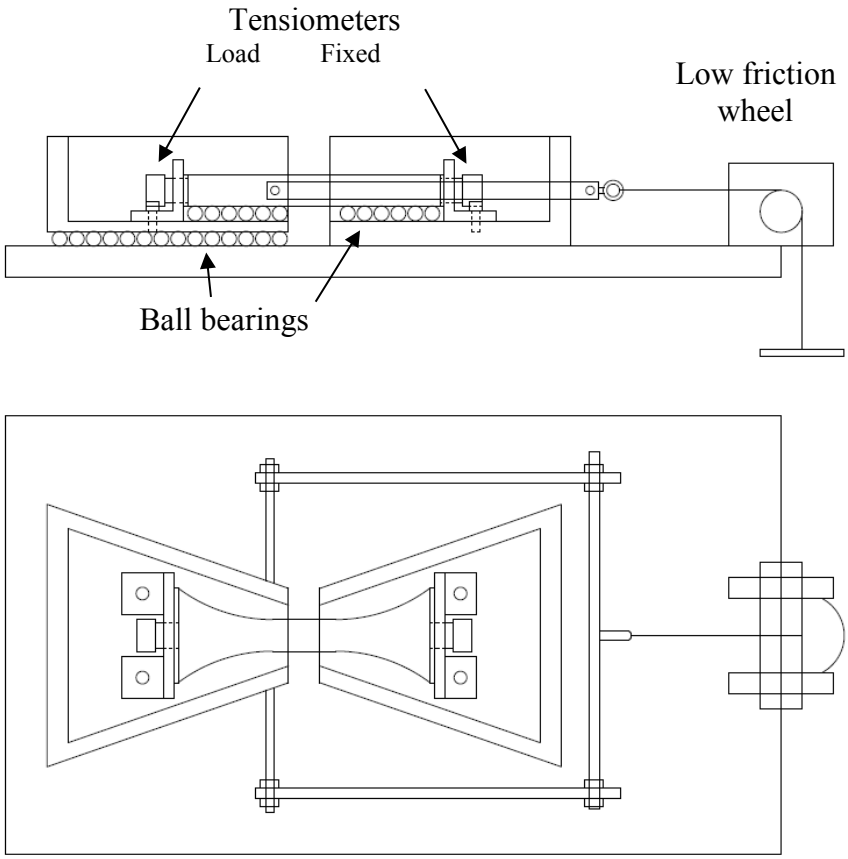

Figure 3 Apparatus for uniaxial compression test

Triaxial cell apparatus

A conventional triaxial apparatus accommodating a 38mm diameter and 76 mm high specimen was used to investigate the response of clays under confined compression. The cell was mounted in a loading frame to apply a constant axial displacement rate during shearing. An internal submersible load cell was used to measure the axial load.

4. EXPERIMENTAL PROCEDURES

Water retention curve

The bar from the slip casting was air-dried to the required gravimetric water content and stored to ensure equilibrium of the water content throughout the soil. A 50 mm diameter metallic cutting ring was used to cut a specimen from the bar. The specimen was placed inside a sealed box and the (negative) pore-water pressure measured using two high-capacity tensiometers (Tarantino 2009). At the end of the measurement, the sample was placed into the oven for 24hrs at 105°c to give the moisture content related to the matric suction.

When the pore-water pressure was beyond the measurement range of the tensiometers, specimens of approximately 1 cm^3 were cut from the cast bar and placed into the WP4C. At the end of the pore water pressure measurement the specimens were placed into the oven for 24hrs at 105°c to give the moisture content related to the total suction.

Because it was not possible to accurately measure the volume of the specimens used for tensiometer and psychrometer measurements, the degree of saturation of the specimens tested was assessed by establishing independently a relationship between degree of saturation and water content along a main drying path. To this end, a cast bar was left to air-dry, and a smaller cutting ring 16 mm diameter and 12.5 mm high was used to cut and trim small specimens at different stages in the drying process from the same bar. The specimen was then placed into the oven for 24hrs at 105°c to obtain the water content. The inner volume of the cutting ring allowed the calculation of the void ratio and hence, the degree of saturation of each specimen.

The combination of these two tests allowed for the relationship between gravimetric water content w, suction s, void ratio e, and degree of saturation S_r to be developed into the

full 'main drying' water retention curve.

The relationships between gravimetric moisture content and degree of saturation and suction for VC and SK are shown in Figure 4 and Figure 5 respectively. Air entry suction values are taken as approximately 450kPa for VC and 700kPa for SK.

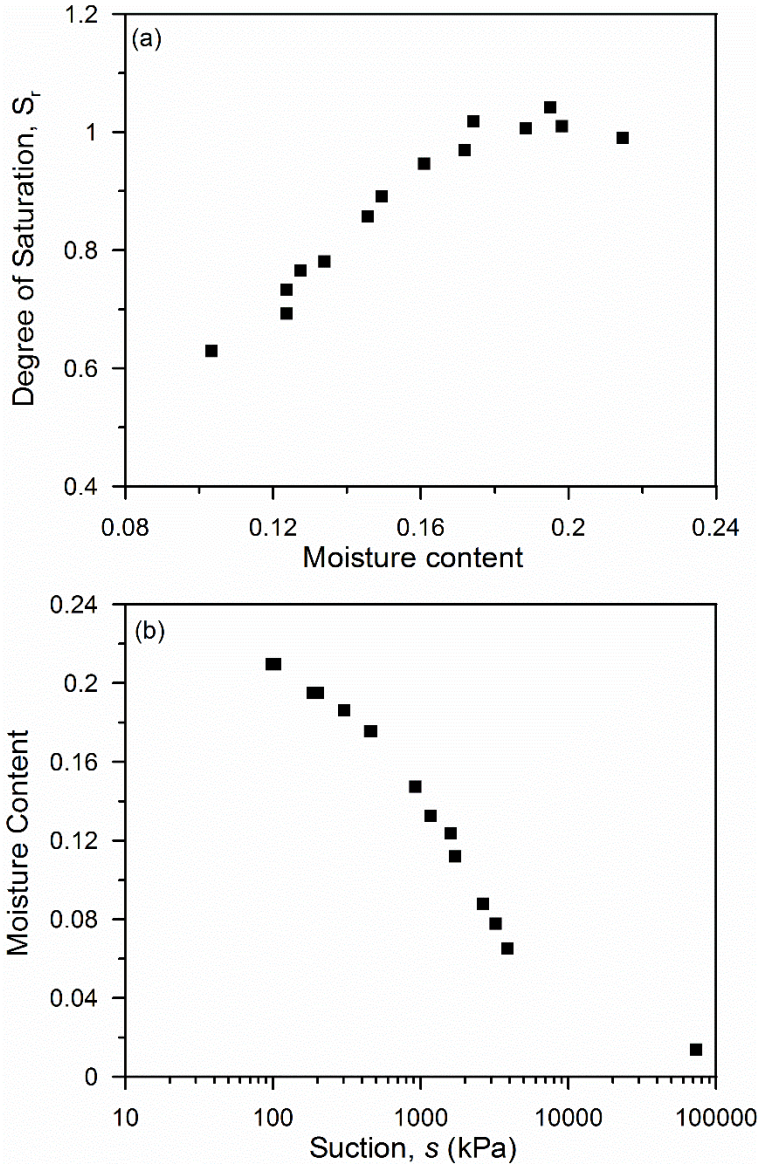

Figure 4 VC material (a) relationship between gravimetric moisture content and degree of saturation (b) relationship between gravimetric moisture content and suction

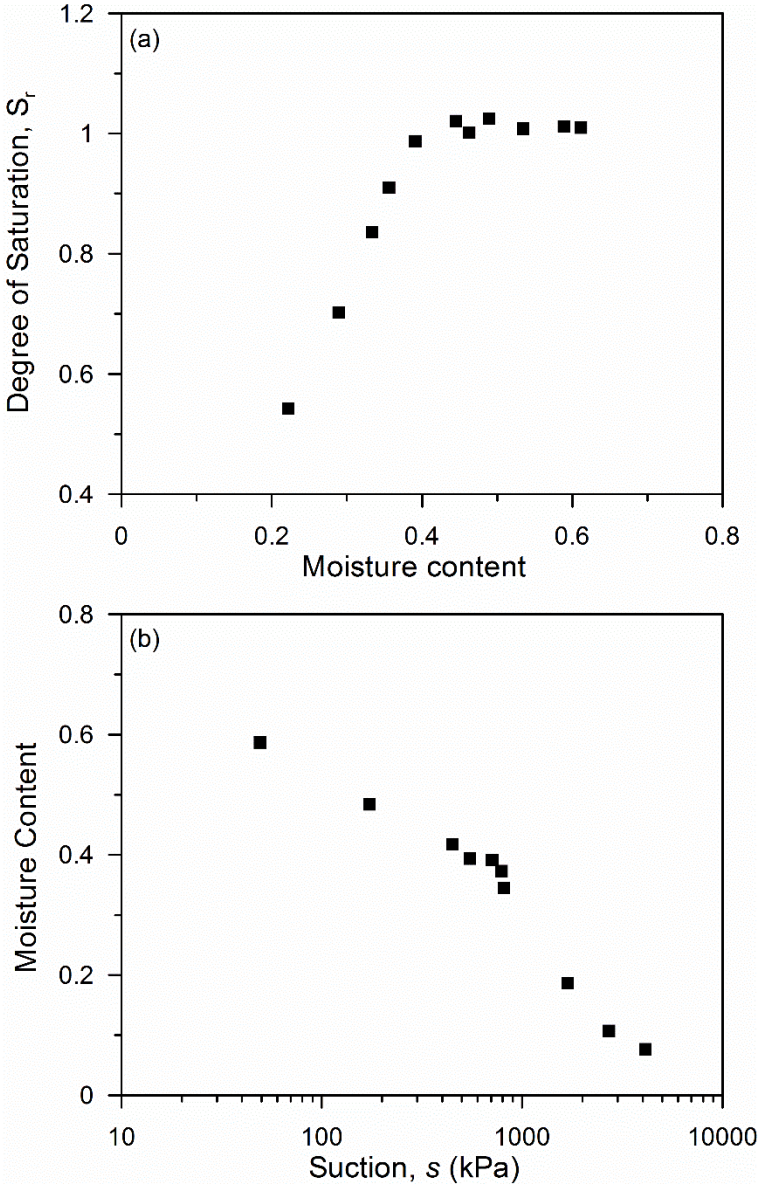

Figure 5 SK material (a) relationship between gravimetric water content and degree of suction (b) relationship between gravimetric moisture content and suction

Tensile test

After removal from the plaster mould, specimens were air dried to the required moisture content and stored for 24hrs. To prevent evaporation, multiple pieces of unstretched plastic paraffin film were used to initially cover the specimen and then grease was used to adhere the pieces of film to each other. The grease did not come into contact with the specimen. Due to

the relatively complex shape of the sample it was not possible to create a completely effective barrier using the film to prevent all evaporation.

The specimen was placed onto the ball bearings and glued to the end restraints. Care had to be taken to align the specimen correctly to the restraints. A plastic wrap was used to prevent evaporation from the holes where the tensiometers would be installed later on and a plastic box was placed over the specimen and equipment. The relative humidity of the air inside the box was raised to help reduce evaporation from the specimen. The specimen was left for 12hrs to allow for the glue to fully cure. After curing the 3 tensiometers were placed onto the specimen and secured. A small amount of soil paste was used to ensure a good contact between the tensiometer and the specimen. The apparatus was again covered with the box while the tensiometers came into equilibrium with the specimen. Prior to loading the plastic box and plastic wrap were removed for a period of one hour to obtain a base evaporation rate. The specimen was loaded axially at a nominal rate of 1.96N/min (≈7 kPa/min) until failure occurred. After failure, a sample from the centre and each of the ends of the specimen was placed into the oven to obtain the gravimetric moisture content at failure.

The loading rate of 7 kPa/min was validated by performing additional tests at a nominal loading rate of 23.5N/min (≈84 kPa/min). As shown in Figure 6, the change in pore water pressure associated with a load step for the two load rates was comparable (when a correction for base evaporation was added). The two tests are also compared in the stress plane (p', q) where p' is the mean effective stress and q is deviator stress under axisymmetric conditions defined here as axial stress minus radial stress. The stress point at failure for the faster load rate specimens was also on the same failure envelope as the tests from the slower load rate indicating that the load rate used had no effect on the test. The 7kPa/min rate was then used for the tests as it allowed the operator easier control during loading.

Due to the centre tensiometer, it was not possible to measure the cross-sectional area of the centre section where the failure was occurring during the tests. The only measurement of size of the centre section possible was to measure the centre section cross sectional dimensions immediately after the sample had ruptured. In order to relate the post rupture area to the area immediately before failure, which is required for the accurate calculation of the stress state at failure, separate tests were performed with the centre tensiometer removed. These tests were performed at three different specimen moisture contents for both the VC and SK soils and a correlation was established between the cross-sectional areas immediately before and after rupture based upon the post failure measured moisture content.

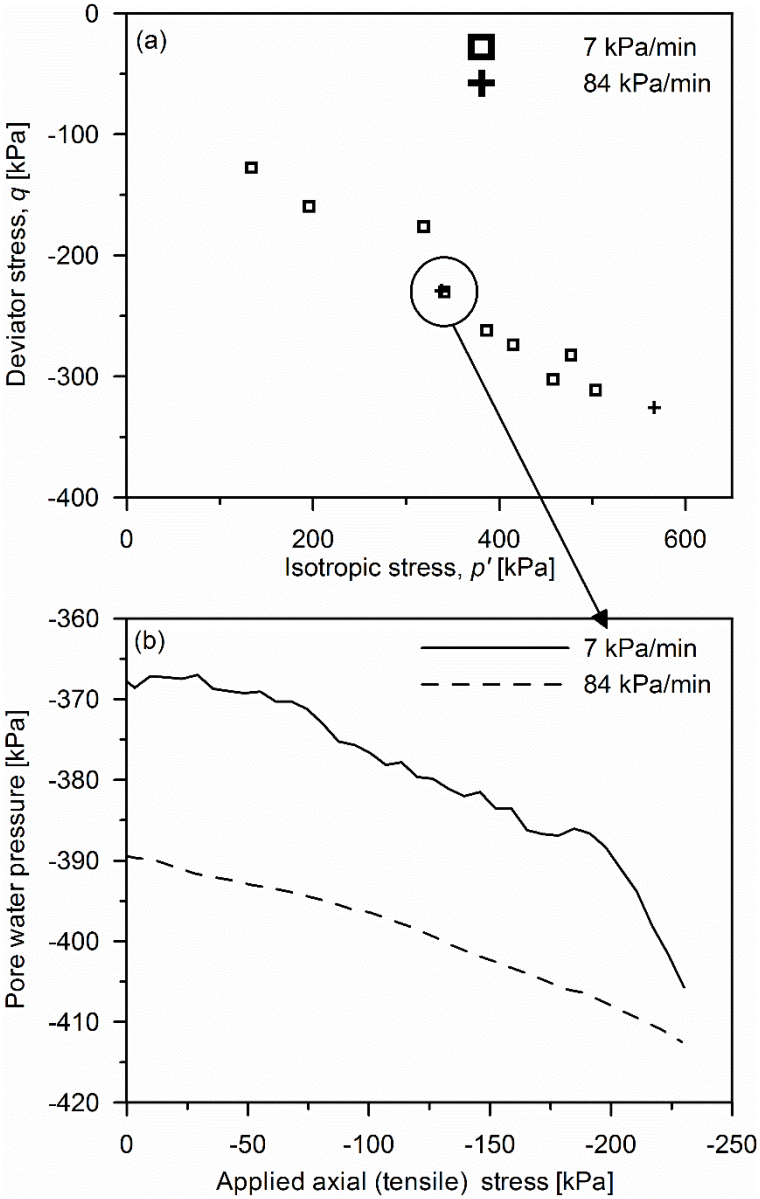

Figure 6 Comparison of uniaxial tension tests performed at different loading rates on VC samples. (a) Shear strength envelope in the plane isotropic effective stress p' versus deviator stress q (b) Evolution of pore-water pressure during shearing for two specimens with similar initial pore water pressures tested at different loading rates

Uniaxial compression test

The same procedure used for the uniaxial tensile test was adopted to glue the specimen to the loading ends and to install the tensiometers. The only exception was the use of petroleum jelly, instead of plastic paraffin film, to cover the specimen during the curing stage. The loading rate for the two tests performed was different, in order to minimise the total test time. The specimen with initial moisture content of 0.197 was loaded in steps of 4.9N (≈15kPa) every 12 minutes. The specimen with initial moisture content of 0.185 was loaded in steps of 19.6N (≈60kPa) every 30 minutes until the stress conditions were equivalent to a friction angle of 20°, then in steps of 9.8N ((≈30kPa) until rupture. The period between loading steps was sufficient to allow the change in the pore water pressure to be similar to that of the baseline evaporation prior to loading. Prior to each increase in load the dimensions of the cross-section of the centre section were measured with callipers. The test was considered to have ruptured correctly if the sample did not bend in any direction prior to failure. After failure, a piece of the centre section was placed into the oven for 24hrs to obtain the moisture content.

Triaxial compression tests

Specimens were cut from the 38mm diameter cast bar to 76mm height and the off-cuts used to obtain the initial moisture content. The specimen was assumed to be saturated when the B-value was greater than 0.95. Specimens were consolidated to an effective isotropic pressure greater than the initial specimen suction calculated from the initial moisture content to ensure that the sample was normally consolidated.

Three tests were performed for both the VC and SK materials, at effective consolidation pressures of 60kPa, 259kPa and 529kPa for the VC and 59kPa, 253kPa and 516kPa for the SK. When the consolidation was complete the drainage valve was closed and the specimens sheared under undrained conditions. An axial displacement rate equal to 0.12mm/minute was imposed for all the tests, with the exception of the 60kPa VC specimen which was tested at 0.07mm/min. Testing was continued until the measured deviator stress no longer increased. The cross-sectional area under loading was calculated according to Head (1986). The cell was then dismantled and the moisture content of the specimen measured.

5. FAILURE BEHAVIOUR OF NON-DE-AIRED SAMPLES IN SATURATED STATE

Vitreous China (VC)

Two uniaxial compression tests under 'quasi-undrained' conditions were carried out on VC samples, having water contents at the start of loading of 19.7 and 18.5% respectively (estimated from the water retention curve and the initial measured suction). Figure 7 shows the evolution of pore-water pressure for the sample tested at w=19.7%. After the installation of the tensiometers, equilibrium was reached after approximately 90 min. The tensiometers then recorded a decrease in pore-water pressure due to the slight evaporation occurring from the sample despite the petroleum jelly coating. The sample was compressed uniaxially at t~240min. Both tensiometers recorded an increase in pore-water pressure with respect to the evaporation baseline. This response is consistent with the behaviour of normally consolidated clay subjected to undrained compression.

The stress paths in the isotropic effective stress p' versus deviator stress q plane for the

two specimens tested in uniaxial compression are shown in Figure 8. At the onset of shearing, the isotropic total stress is equal to zero and the pore-water pressure is negative giving rise to a positive isotropic effective stress. The same figure also shows the stress paths for the specimens subjected to conventional CU triaxial compression test where the total stress is equal to the cell pressure and the pore-water pressure is positive at the onset of shearing, giving rise again to a positive isotropic effective stress. Table 1 summarises the conditions of the samples at the start of shearing for the uniaxial compression and triaxial compression tests for both materials, where p'_0 is the initial effective mean stress.

The stress data points at the critical state form a linear envelope passing through the origin, corresponding to a gradient, M_c, as would be expected for a soil reconstituted from slurry. The corresponding critical state friction angle is φ'_{cs}=27.8°, calculated from:

$$\sin\varphi' = \frac{3M_c}{6 + M_c} \qquad [1]$$

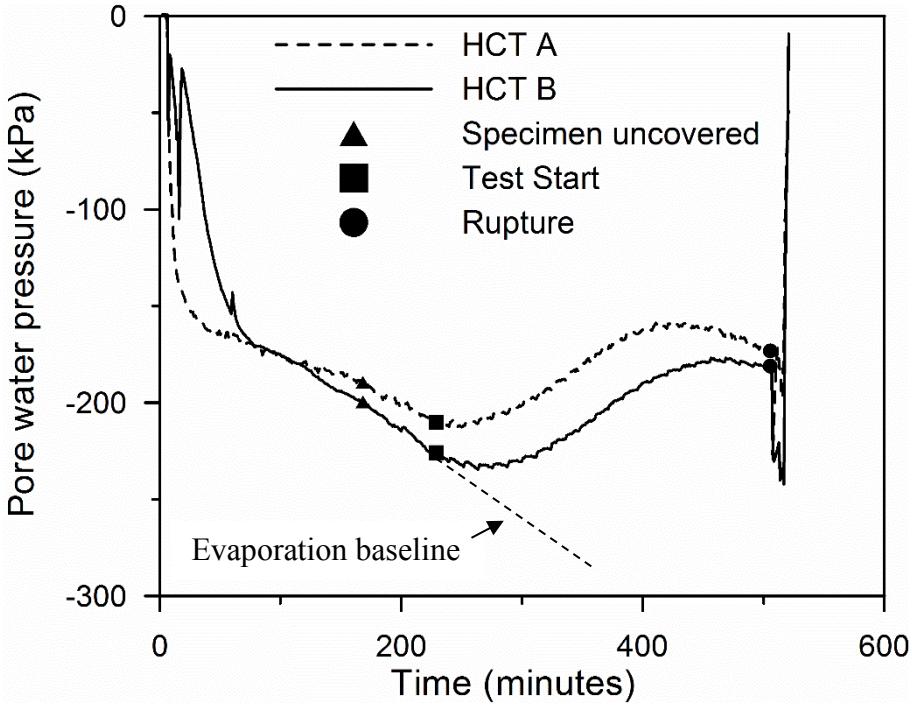

Figure 7. Evolution of pore-water pressure measured by the HCTs during the uniaxial compression test on VC (w=19.7%).

Figure 8 also shows the critical state data in the compression plane together with the normal consolidation line (*ncl*) obtained from samples air-dried to target water content with suction measured using the tensiometers. The critical state data for the specimens tested in triaxial compression are located below the *ncl* as expected. On the other hand, the water content of the specimens tested in uniaxial compression were unexpectedly above the *ncl*. This was attributed to a water exchange during loading with the petroleum jelly coating, which was removed from the specimen before being placed in the oven. For this reason, no petroleum jelly coating was used in the subsequent tensile tests.

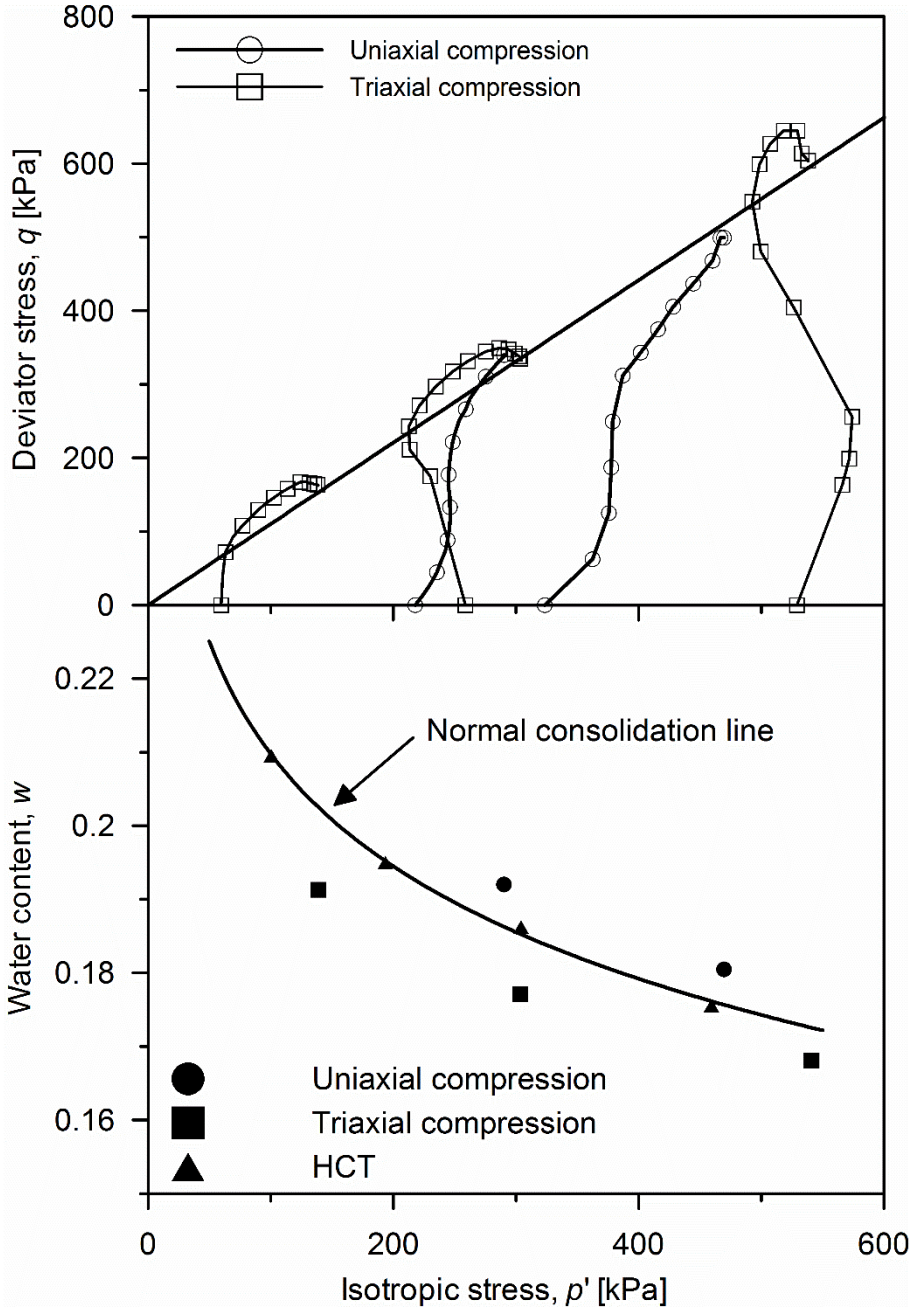

Figure 8 Stress-paths and water contents at failure for uniaxial and triaxial compression tests for VC

Table 1 Initial conditions for uniaxial compression and triaxial compression tests

	VC		SK	
	W_0 (%)	p'_0 (kPa)	W_0 (%)	p'_0 (kPa)
UC 1	19.7	218	-	-
UC 2	18.5	323	-	-
Triaxial 1	19.1	60	51.4	59
Triaxial 2	17.7	259	47.6	253
Triaxial 3	16.8	529	40.7	516

Nine uniaxial tension tests under 'quasi-undrained' conditions were carried out on VC specimens having initial water contents ranging from 20% to 17%. The initial water contents were calculated using the initial pore water pressures recorded by the tensiometers. All these samples were tested under saturated conditions. Figure 9 shows the evolution of pore-water pressure for the sample tested at w=17.7%. After the installation of the three tensiometers (two at the ends and one in the middle), equilibrium was reached after about 120 min. To ensure that proper equilibrium was reached with the tensiometers, water evaporation was prevented by using plastic paraffin film, plastic wrap and a box as described previously.

At t~200min, the plastic wrap and box were removed (leaving the plastic paraffin film layer in place) and a slight decrease in pore-water pressure was observed due to the slight evaporation occurring from the sample. This decrease in pore-water pressure was significantly less than the one observed on samples tested in uniaxial compression (Figure 7) due to the better insulation system created by the plastic paraffin film. The specimen was finally subjected to a tensile uniaxial stress t≈260 min. The three tensiometers showed consistent

measurement and recorded a decrease in pore-water pressure upon tension.

The tensiometer installed in the centre section of the specimen recorded a greater decrease in pore-water pressure than those at the ends and this has been the typical response for the majority of the tests. The pore-water pressure recorded by the centre tensiometer was then used to quantify the changes in isotropic effective stress during the tensile test, the other two tensiometers were used to check the consistency of the measurement of the centre tensiometer.

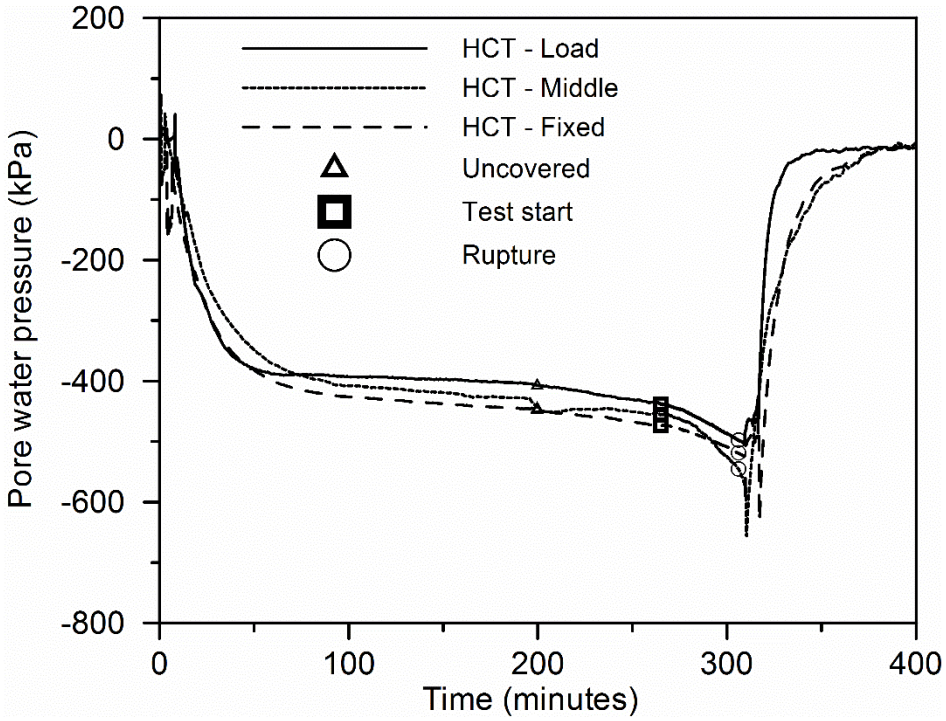

Figure 9 Evolution of pore-water pressure measured by the HCTs during the uniaxial tension test on non-de-aired VC (Test 21-10).

The stress paths for the non-de-aired VC uniaxial tension tests in the *p*'-*q* plane are shown in Figure 10 together with the critical state line from the triaxial and uniaxial

compression tests converted from compression to extension. It has been assumed that the soil is characterised by a unique friction angle, φ', in extension and compression, which leads to a slope of the critical state line in extension, M_e, given by:

$$M_e = \frac{6sin\varphi'}{3 + sin\varphi'} \quad [2]$$

It can be observed that only the two specimens with low suctions reach the failure envelope. For all the remaining specimens, the failure data point at rupture lie above the critical state line, i.e. they failed at lower tensile uniaxial stress. A similar response was observed in the volumetric plane. The two specimens at low suction match reasonably well with the critical state line derived from triaxial compression tests, whereas the other specimens generally appear to lie between the *ncl* and *csl*.

Speswhite kaolin (SK)

Only CU triaxial compression tests could be performed on SK specimens. Uniaxial compression tests were attempted but none were successful due to bending of the specimen upon uniaxial compression. Three samples were tested in triaxial compression having a suction of ~150 kPa after removal from mould. These samples were subjected to a confining effective stress of 59, 252, and 516 kPa respectively. As a result, the sample subjected to the lowest effective confining pressure was slightly over-consolidated whereas the other two were normally consolidated at the onset of shearing.

The stress data points at the critical state were fitted using a linear envelope passing through the origin as shown in Figure 11. The corresponding critical state friction angle is

φ'_{cs}=23.5°.

Figure 11 also shows the critical state data in the volumetric plane together with the normal consolidation line (*ncl*) obtained from samples air-dried to target water content with suction measured using tensiometers. The critical state data for the specimens tested in triaxial compression are located below the *ncl* as expected.

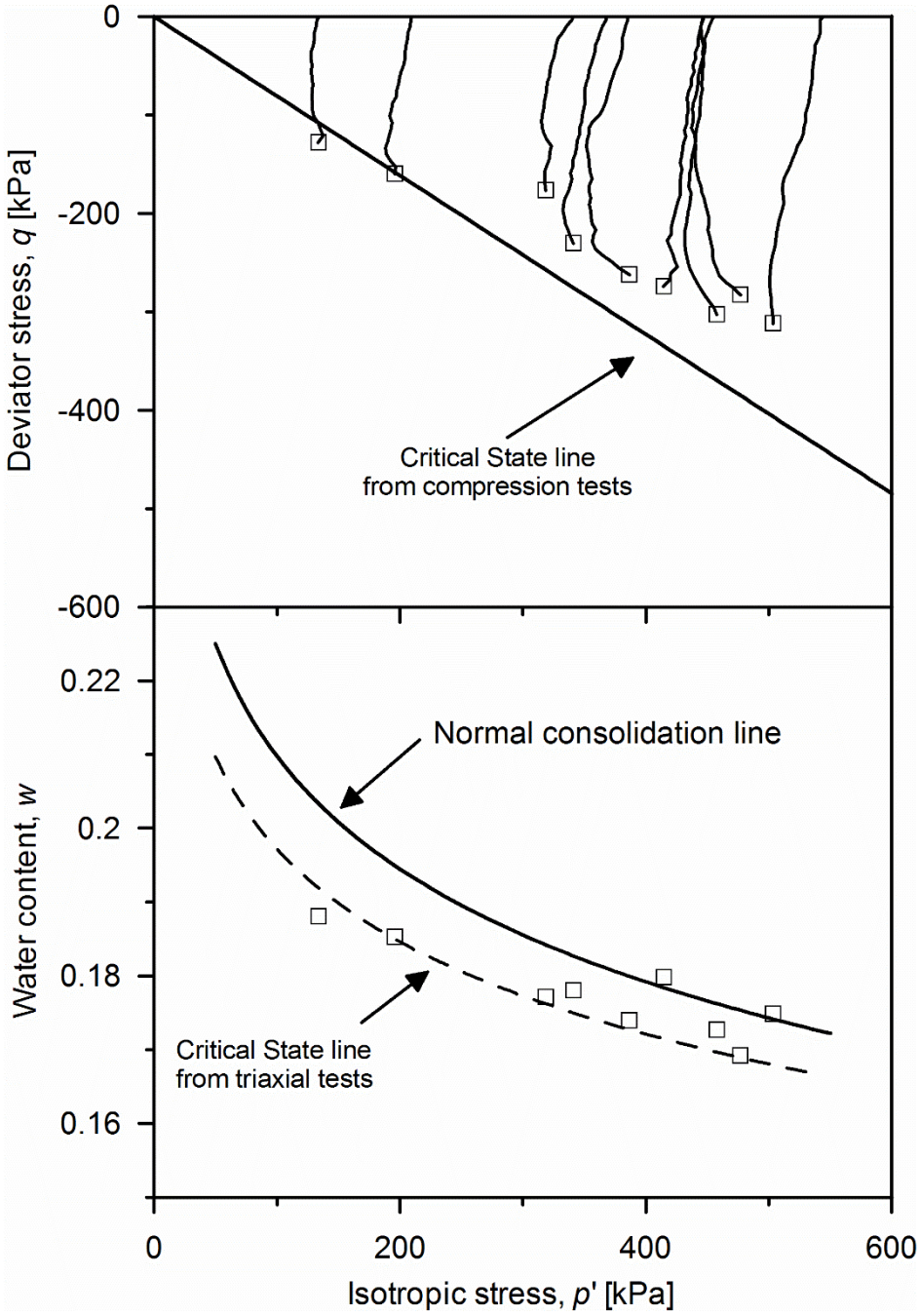

Figure 10 Stress-paths and water contents at failure for uniaxial tension tests for non-de-aired VC

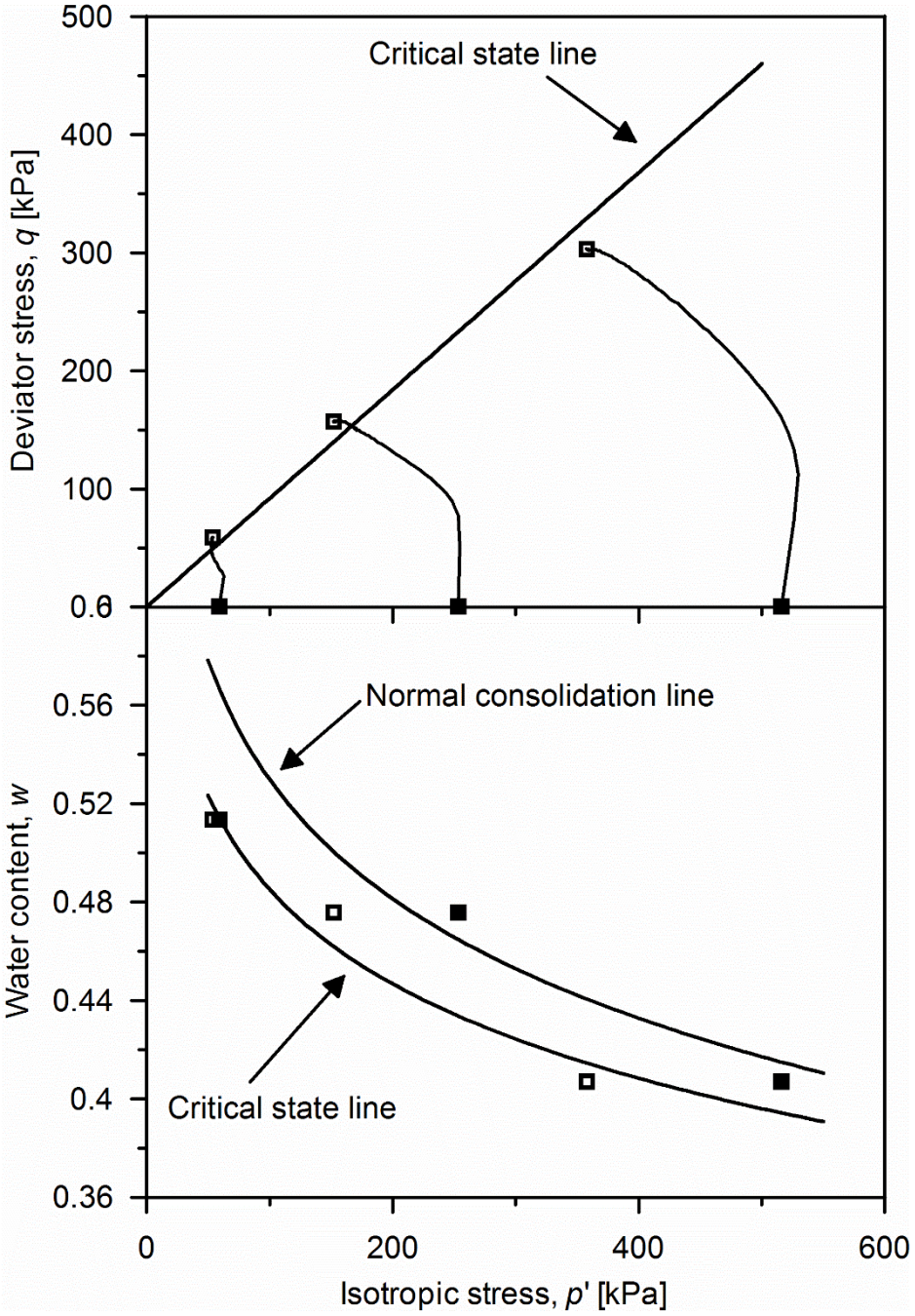

Figure 11 Stress-paths and water contents at failure for uniaxial and triaxial compression tests for SK

The stress paths in the *p*'-*q* plane for the SK uniaxial tensile tests are shown in Figure 12 along with the critical state line derived from the friction angle taken from triaxial compression tests. It can be observed that most of the specimens tested in uniaxial tension are

reaching the same critical state derived from the triaxial compression tests line, except from the three specimens at high suction (closer to the air-entry suction but still in the saturated range) where the failure data point at rupture lies above the critical state line, i.e. they failed at lower tensile uniaxial stress. It can also be observed that two samples with low initial suction, fail below the CSL. These samples were tested just after removal from the plaster mould without subjecting the specimens to any further air-drying. In the plaster mould, suction is higher at the outer boundary of the specimen than it is in its inner part. Water content redistribution after removal from the plaster mould would perhaps leave the specimen in a slightly overconsolidated state. This would explain failure at deviator stress lower than the peak and close to failure in tension, i.e. zero minor principal effective stress. This overconsoldiated state would be erased when specimens are brought to higher suction and, hence, isotropic effective stress upon air-drying.

6. FAILURE BEHAVIOUR OF DE-AIRED SAMPLES IN SATURATED STATE

Tensile test data on Vitreous China (VC) and Speswhite Kaolin (SK) have shown that the rupture of the specimens is i) associated with failure in shear and ii) the critical state lines do not appear to be significantly different from the ones inferred from triaxial and uniaxial compression tests. However, it was observed that failure data points depart from the critical state line as the suction approaches the air-entry value, i.e. specimens fail at a tensile stress lower than the one predicated by the critical state line inferred from compression tests. Although all specimens were tested in the saturated range, it was speculated that small air cavities could expand in the soil when suction approaches the air-entry value. When the specimen is pulled under undrained conditions, suction increases and some air cavities would rapidly expand (cavitation) causing a local a drop in water tension and, hence, in confining

effective stress. This would trigger failure in shear locally that would then propagate across the entire cross section.

To corroborate this assumption, tests on VC and SK specimens were prepared after de-airing the slurry. This was expected to reduce the amount of air present in the pore-water in the form of tiny undissolved air cavities (cavitation nuclei) and, hence, to reduce the susceptibility of the pore-water to cavitation.

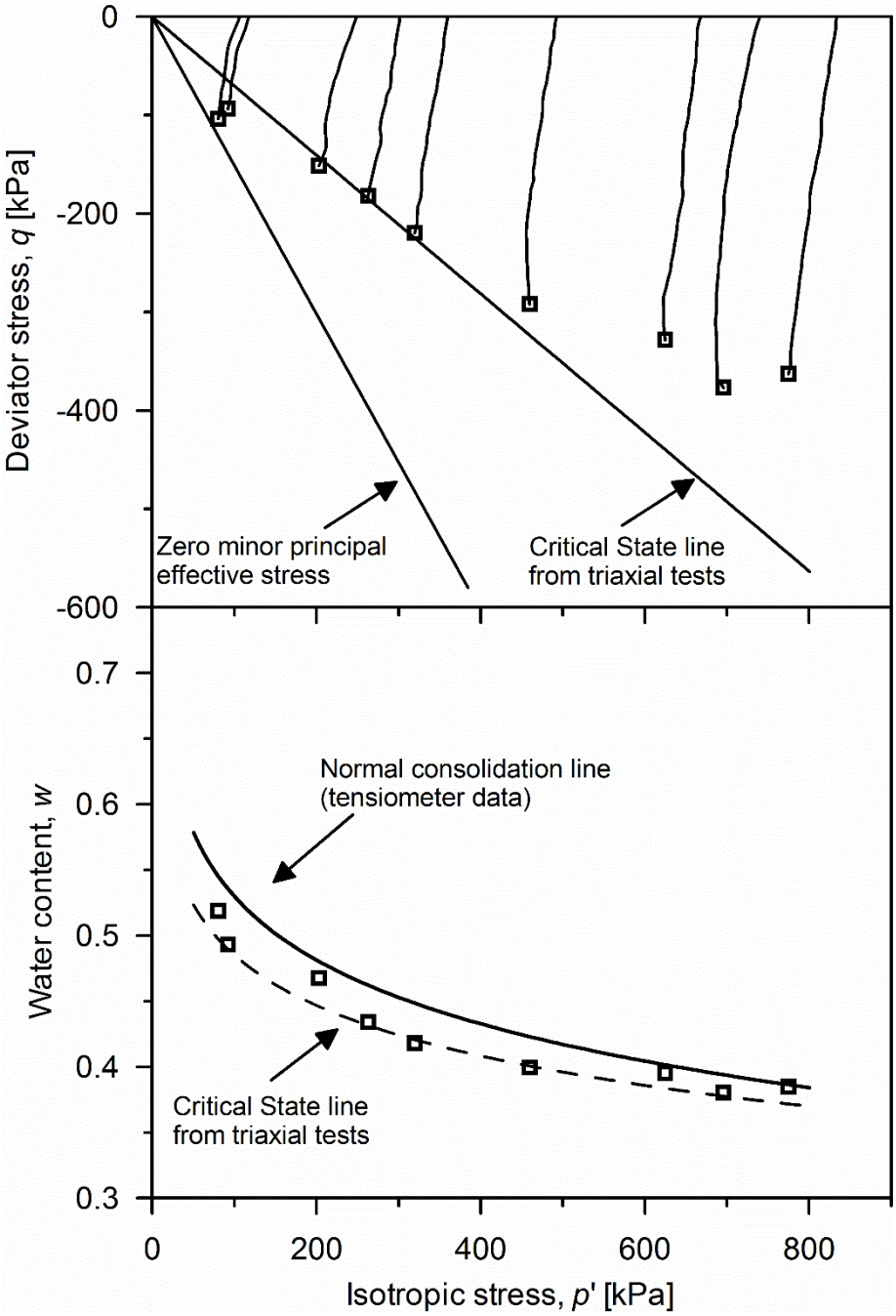

Figure 12 Stress-paths and water contents at failure for uniaxial tension tests for non-de-aired SK

The results from tensile tests on de-aired specimens of VC are shown Figure 13. The critical state data for the non-de-aired specimens are also shown for comparison. It can be observed that around 50% of the failure data points for the de-aired specimens in the *p*'-*q*

plane lie on the critical state line. Similarly, data points for de-aired samples in the *p*'-*w* plane are better aligned with the critical state line than non-deaired samples.

The results from tests on de-aired specimens on SK are shown in Figure 14. Although the data from de-aired specimens are not falling in the same range of the non-de-aired specimens at high suction that depart from the critical state line, there seems to be similar tendency for de-aired specimens to remain closer to the critical state line than non-de-aired specimens.

It is interesting to explore whether the tensile failure pattern corroborates the finding that tensile failure occurs in shear. Figure 15 shows the theoretical angle between the planes of failure and the minor principal plane. The typical tensile failure pattern observed in uniaxial tensile VC and SK samples are shown in Figure 16 and appear to be consistent with a shear failure mode (mixed Mode I and Mode II fracture).

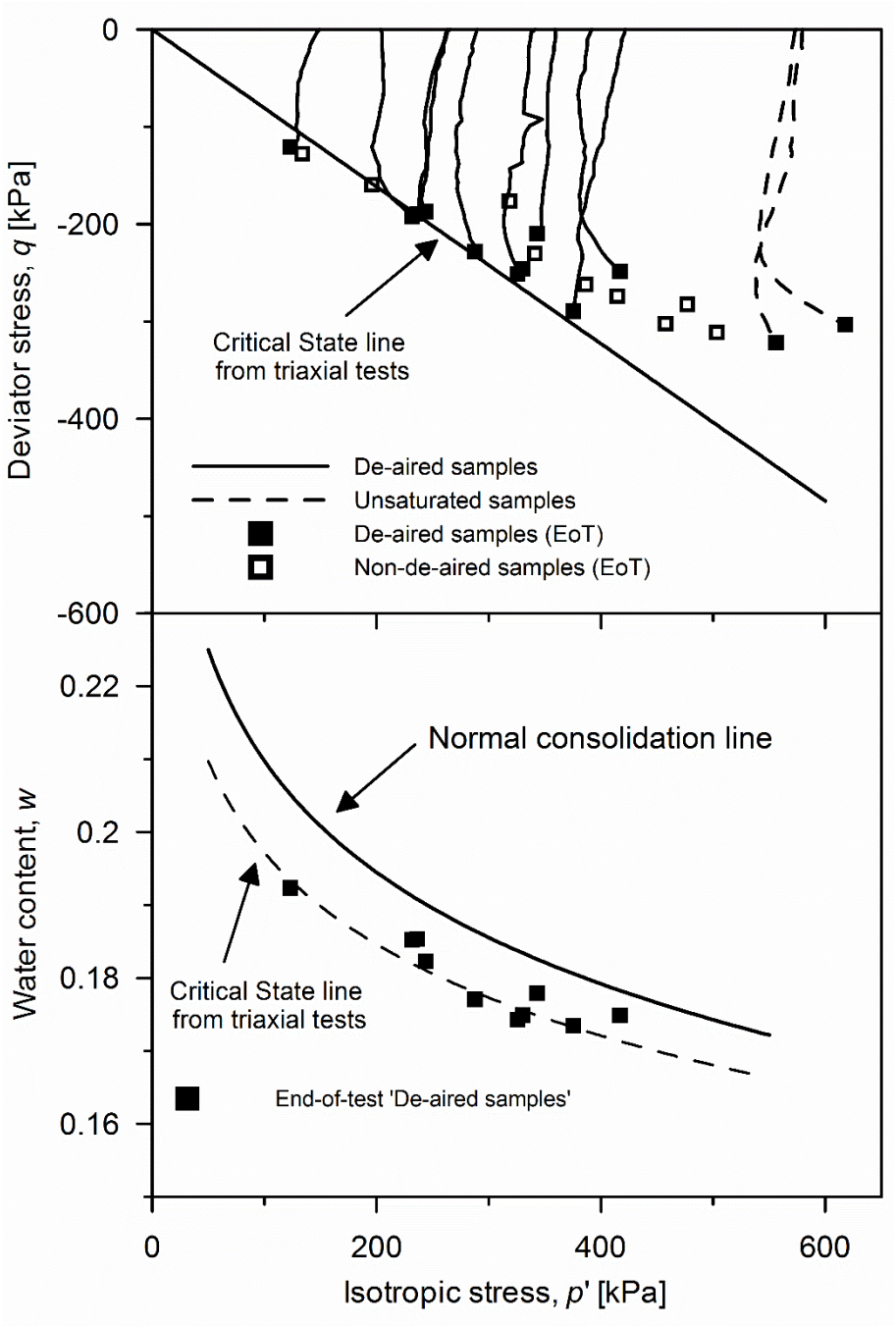

Figure 13 Stress-paths and water contents at failure for uniaxial tension tests for -de-aired VC

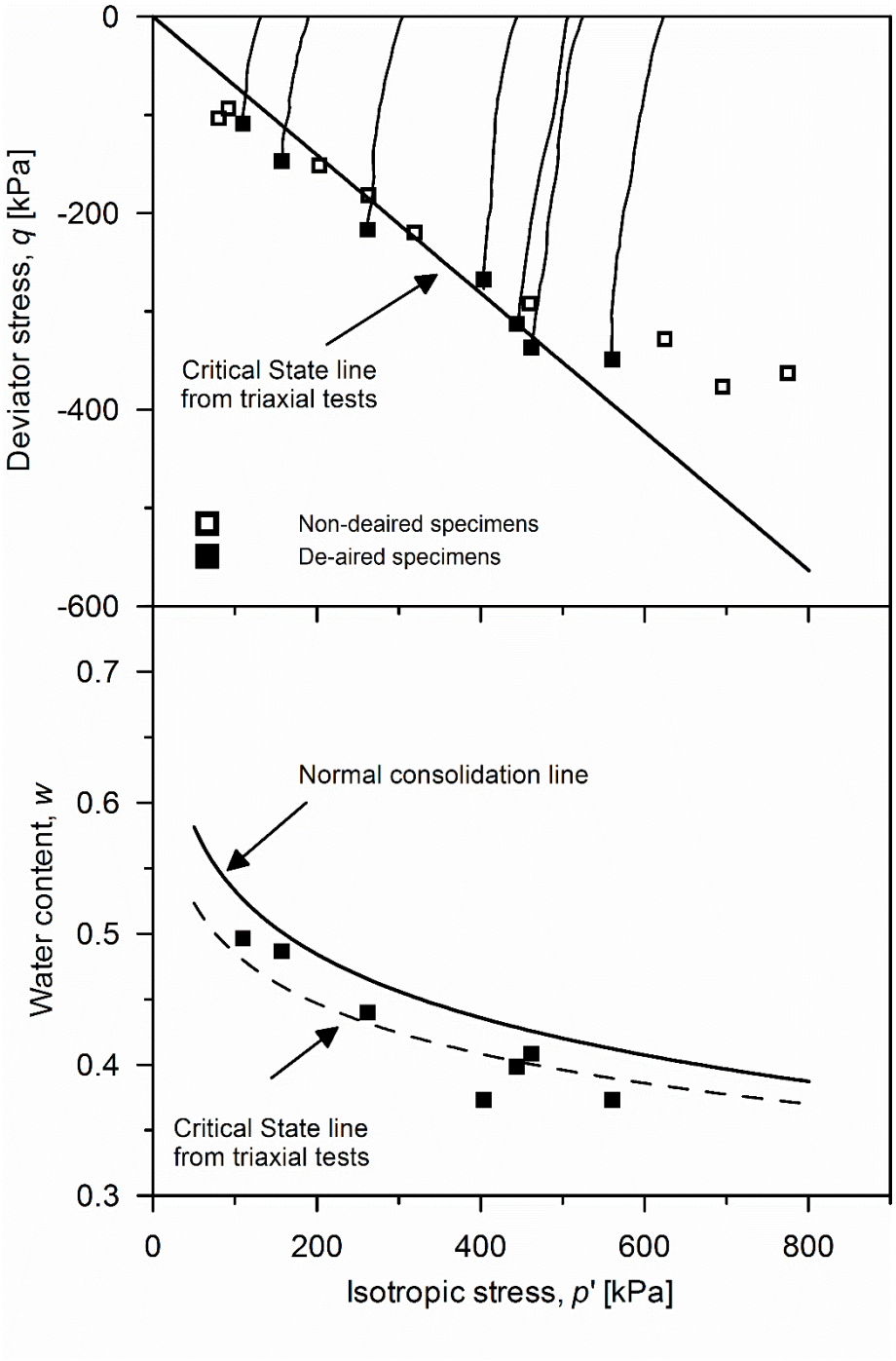

Figure 14 Stress-paths and water contents at failure for uniaxial tension tests for -de-aired SK

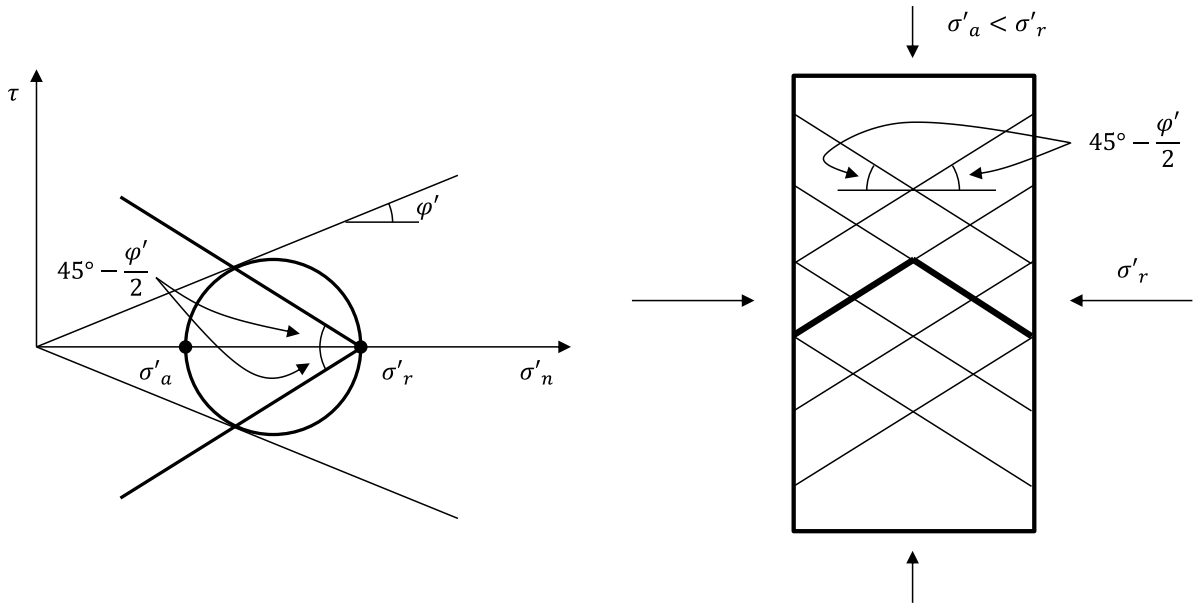

Figure 15 Theoretical angle between planes of failures and minor principal plane

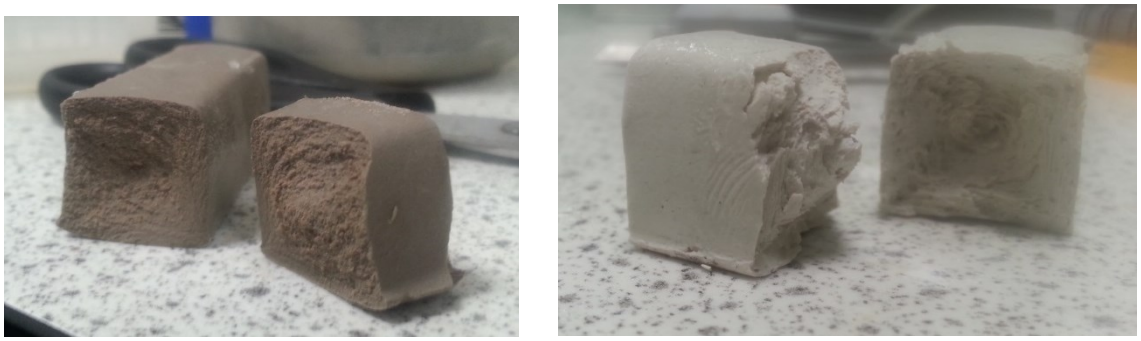

(a) (b)

Figure 16 Tensile failure patterns in de-aired samples. (a) VC and (b) SK

7. FAILURE BEHAVIOUR OF SAMPLES IN UNSATURATED STATE

Six specimens of VC were tested in the unsaturated range, one prepared from non-de-aired slurry and the other five prepared from de-aired slurry.

Since tensile test data in the saturated range could be fitted by a traditional Mohr-

Coulomb failure criterion, it was tentatively assumed that data in the unsaturated range could also be modelled by extending the Mohr-Coulomb criterion to the unsaturated range.

The criterion proposed by Vanapalli et al. (1996) and validated by Tarantino and El Mountassir (2013) for a wide range of clayey geomaterials was considered here:

$$q = M(p + s \cdot S_r^k) \qquad [3]$$

where M is the 'saturated' critical state parameter, p is the isotropic total stress, s is the suction, S_r is the degree of saturation, and k is a scaling parameter for the degree of saturation. This failure criterion requires the parameter k to be derived by the best-fitting of data points in the unsaturated range. To this end, the degree of saturation at failure needs to be estimated for the tensile tests performed in this programme.

Since the void ratio at failure could not be measured, the degree of saturation could not be determined directly, and a different route was pursued. At the onset of shearing, unsaturated specimens lie on a main-drying surface in the space (s, e, e_w), where s is the suction, e is the void ratio, and e_w is the water ratio. Upon shearing, the void ratio increases at constant water content. The degree of saturation therefore keeps decreasing and moves along a main-drying surface. If an equation is derived for the main drying surface, the degree of saturation at failure can be inferred from the main drying surface and from the measurement of s and e_w at failure.

Tarantino (2009) proposed and validated a model for a water retention surface in the space (s, e, e_w):

$$S_r = \frac{e_w}{e} = \left\{ 1 + \left[\left(\frac{e}{a} \right)^{\frac{1}{b}} s \right]^n \right\}^{-\frac{b}{n}} \quad [4]$$

where S_r is the degree of saturation, a and b are two parameters derived explicitly from experimental data at very high suction in the plane (s, e_w) and n is an additional parameter to be determined by best fitting. Water retention data for values of high suction in the plane (s, e_w) are plotted in Figure 17, where they are interpolated by a straight line in a log-log plot. The parameters of the power function are directly associated with the parameters of the main drying surface (a=16.231, b=0.544). The last parameter was determined by best fitting as shown in Figure 18. Two possible values for n are shown in the figure, n=3 and n=4. The overlap between the tensiometer and WP4C data show that the osmotic suction for the VC material is negligible.

Once the parameters of the main drying surface were determined, the void ratio and, hence, the degree of saturation at failure could be derived from Eq. [4] for given values of suction and water ratio at failure. Eq. [3] can be therefore be used to predict the deviator stress at failure for specimens tested under unsaturated conditions.

The tensile stress test data versus suction (at failure) for the six unsaturated specimens is shown in Figure 19 together with the tensile stress data for the saturated specimens prepared from de-aired slurry. The performance of the shear strength model given by Eq. [3] is shown in Figure 19 for two values of the water retention parameter n (k=2.2). It can be observed that tension data can be reasonably fitted by a shear strength model, confirming that tensile failure is associated with failure in shear even for unsaturated specimens.

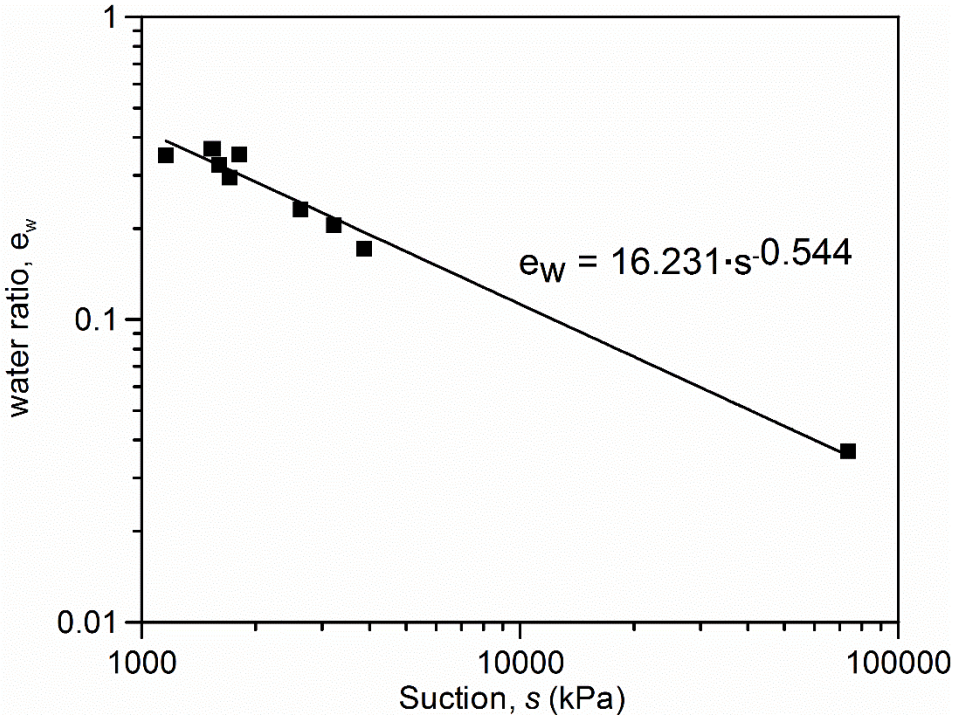

Figure 17 Vitreous China water retention drying data at high suction

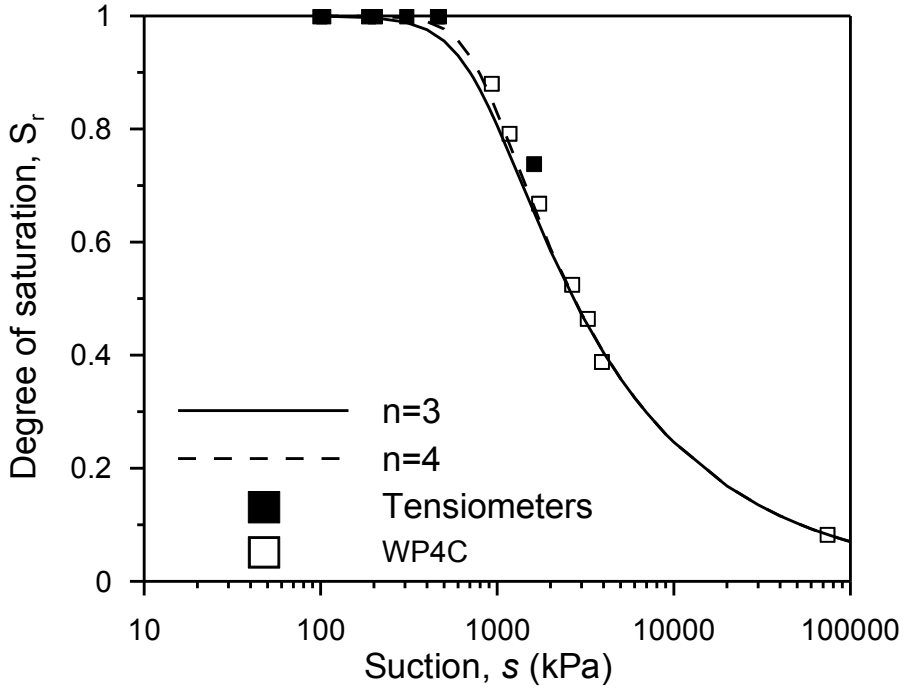

Figure 18 Vitreous China water retention drying curve

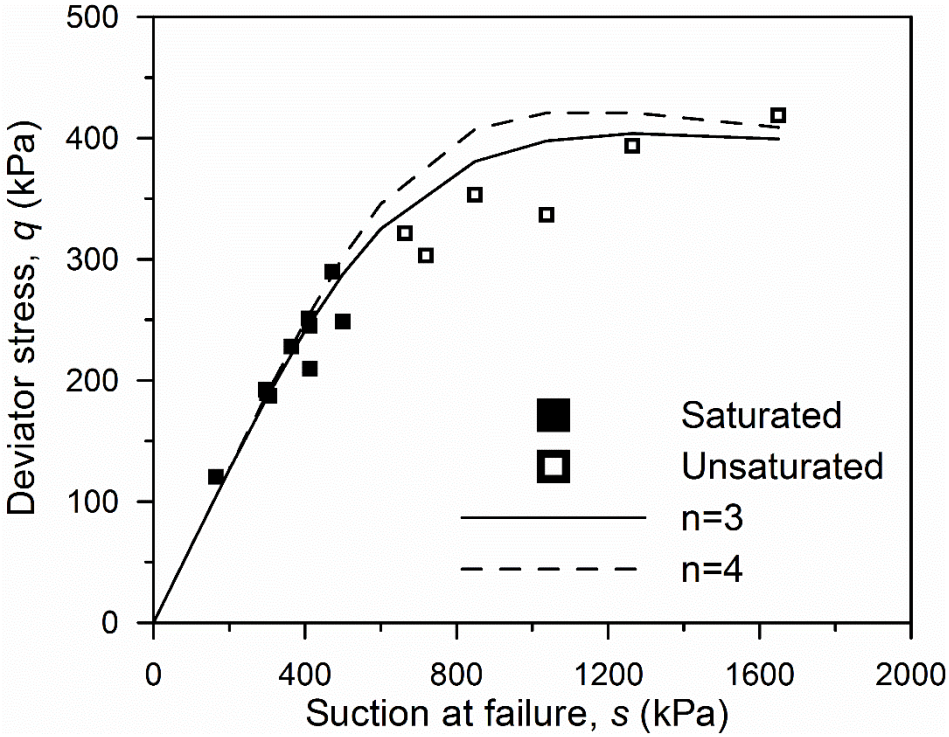

Figure 19 Failure data points for saturated (de-aired) and unsaturated specimens and failure envelopes for two different values of the water retention parameter n.

8. DISCUSSION

The results from uniaxial tensile tests performed on samples prepared with de-aired water (Figure 13 and Figure 14) have suggested that cavitation occurring at suction below the air-entry value can trigger early rupture of the specimen.

The possible interplay between the formation of cracks in clay and the process of cavitation has been already suggested by Haigh et al. (2013). In particular, they have assumed that the cracks appearing within the soil thread during the plastic limit test may result from an expansion of cavitation nuclei until the gas occupies the entire cross-section of the thread and the water tension can no longer be transferred through the fluid.

Although Haigh et al. (2013) gave convincing arguments in support of this hypothesis, no

direct experimental evidence was provided. Based on the lesson learned from the uniaxial tests performed in this programme, a difference in the plastic limit would be expected depending on whether de-aired or non-de-aired water is used to prepare the clay thread. In particular, if cavitation is not occurring, a higher suction and, hence, a lower water content could be reached before cracks appears in the clay thread. In other words, preparing the clay with de-aired water should decrease the water content at the apparent plastic limit.

Plastic limit tests were therefore performed on the SK and VC mixes. Two bars of each soil type were cast: one using de-aired slip and the second with normal slip. The plastic limit tests were performed in accordance with BS 1377-2. While performing the plastic limit tests the operator did not know if it was soil that had been de-aired or non-de-aired to prevent any operator bias from affecting the results. Eleven tests were performed on each bar type.

The results of the plastic limit tests are shown in Figure 20 for both VC and SK mixes. Data are presented in terms of cumulative distribution, i.e. the probability that the plastic limit is lower than the value read on the horizontal axis. It can be clearly seen that the cumulative distributions shifts to the left (towards lower water contents) for the case where specimens are prepared with de-aired water. The average plastic limit reduced by Δw=0.5 for the VC and Δw=1.7 for the SK.

These results provide further evidence of the role played by cavitation on crack formation and corroborates the mechanism postulated by Haigh et al. (2013).

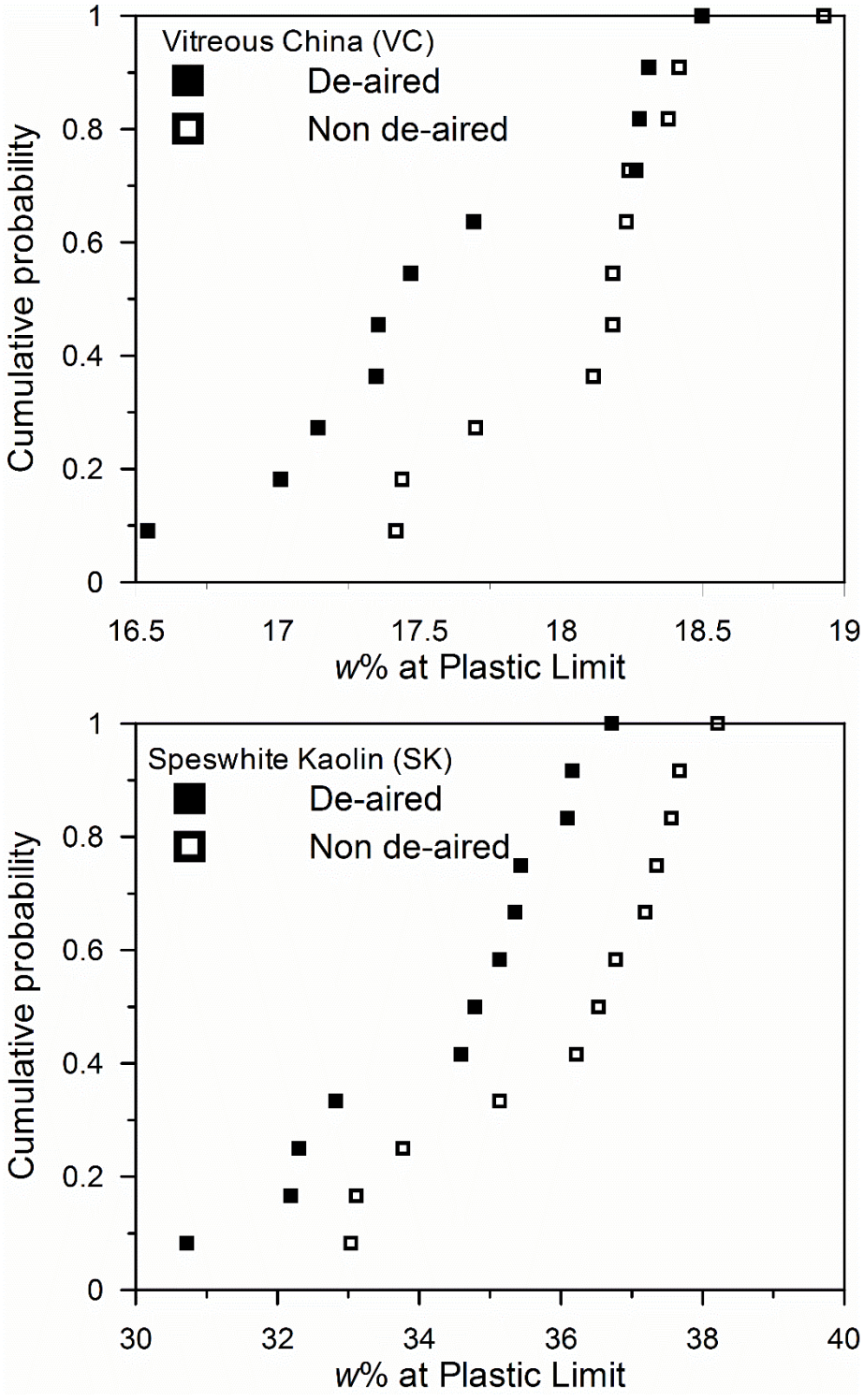

Figure 20 Plastic limit tests de-aired and non de-aired specimens of VC and SK

9. CONCLUSIONS

The paper has presented an experimental investigation of the mechanisms of tensile failure in clayey geomaterials under saturated and unsaturated conditions. To this end, an experimental apparatus was developed to test specimens in uniaxial tension with the facility to monitor suction using high-capacity tensiometers. This allowed interpretation of the data to be done in terms of effective stress for the saturated specimens and in terms of average skeleton stress for the unsaturated specimens.

The first series of test was performed on saturated samples of Vitreous China clay and Speswhite kaolin clay. Samples were reconstituted from slurry (prepared by slip-casting) and prepared using non-de-aired water. When suction approached the air-entry value, failure occurs at a deviator stress lower than the one corresponding to the critical state line derived from triaxial and uniaxial compression. This behaviour was observed for both of the clays tested.

Although all specimens were tested in the saturated range, it was speculated that small air cavities could develop in the soil when suction approaches the air-entry value. When the specimen is pulled under undrained conditions, suction increases and some air cavities would rapidly expand (cavitation) causing a local a drop in water tension and, hence, in confining effective stress. This would trigger failure in shear locally that would then propagate across the entire cross section. To probe this assumption, a second series of tests were performed on saturated specimens with the slurry preventatively de-aired before slip casting. The de-airing process was aimed at reducing the number of cavitation nuclei the clay and, hence, at reducing the probability of early failure due to water cavitation. Indeed, the de-airing process realigned the deviator stress at failure recorded in the tensile test with the critical state line derived from uniaxial and triaxial compression tests. This seems to support the assumption

that water cavitation may control premature rupture of clay when subjected to a (total) tensile stress state. Failure data on unsaturated specimens could also be fairly modelled by the Mohr-Coulomb criterion extended to unsaturated states (by replacing the effective stress for saturated geomaterials with the average skeleton stress). This suggests that tensile failure is associated with failure in shear in both saturated and unsaturated state. The observation of the tension crack pattern appears to be consistent with a combined Mode I and Mode II fracture.

ACKNOWLEDGEMENTS

The authors wish to thank Ideal Standard International and EPSRC via a Doctoral Training Grant for supporting the research. They also wish to thank Fernando Francescon from Ideal Standard Italia s.r.l. for his helpful discussions, Derek McNee for his help constructing the test apparatus, and Arianna Gea Pagano and Elena Prato for their assistance with the triaxial tests.

10. REFERENCES

Ajaz, A., & Parry, R.H.G. 1975. Stress-strain behaviour of two compacted clays in tension and in compression. *Geotechnique*, 25(3): 495-512.

Albrecht, B.A. & Benson, C.H. 2001. Effect of desiccation on compacted natural clay. *J Geotech Geoenviron Eng,* 127, No. 1, 67–75.

Alonso, E.E., Pereira, J.M., Vaunat, J., and Olivella, S. 2010. A microstructurally-based effective stress for unsaturated soils. *Géotechnique*, 60(12): 913–925.

Amarasiri, A.L., Kodikara, J.K. & Costa, S. 2011. Numerical modelling of desiccation cracking. *Int J Numer Anal Methods Geomech*, 35, No. 1, 82–96.

Ávila, G. (2004). Study on the cracking behaviour of clay. Application to Bogota clay. Ph.D. Thesis, Technical University of Catalonia, Barcelona, Spain.

Baker, R. 1981. Tensile strength, tension cracks and stability of slopes. *Soils and Foundations,* 21, No. 2, 1–17

Bowman, JR. 1926. Recent Factory Experience and Experiments in Drying Terra Cotta, *J. Am. Ceram. Soc*, 9, No. 6, 380–91.

Clews, H. 1969. Heavy Clay Technology. Academic Press, New York.

Cooper, A.R. 1978. Quantitative theory of cracking and warping during the drying of clay bodies. In Ceramic Processing Before Firing, GY Onoda and LL Hench (eds). John Wiley & Sons, New York.

Marnette, E. , Schuren, C. , van de Brink, K., Glew, N.D. and Dyer, M. (2006) Further tests on the fissuring of clay fill at thorngumbald food embankment. In: Advanced Experimental Unsaturated Soil Mechanics: Experus 2005. Taylor and Francis Group, London, United Kingdom, pp. 501-504. ISBN 9780415383370

Greve, A., Andersen, M. & Acworth, M. 2010. Investigations of soil cracking and preferential flow in a weighing lysimeter filled with cracking clay soil. *J Hydrol*, 393:105–13.

Haigh, S.K., Vardanega, P.J. & Bolton, M.D. 2013. The plastic limit of clays. *Geotechnique,* 63, No. 6, 435-440.

Handy, R.L. & Lustig, M. 2017. Tension Cracks in a Compacted Clay Embankment. *Journal of Geotechnical and Geoenvironmental Engineering*. 143. 06017006. 10.1061/(ASCE)GT.1943-5606.0001667.

Head, K.H. 1986. Manual of Soil Laboratory Testing. Pentech Press, London.

Heibrock G., Zeh R.M., Witt K.J. 2005. Tensile Strength of Compacted Clays. In: Schanz T. (eds) Unsaturated Soils: Experimental Studies. Springer Proceedings in Physics, vol 93. Springer, Berlin, Heidelberg

Houlsby, G. T. (1997). The work input to an unsaturated granular material. *Geotechnique* 47, No. 1, 193–196.

Hughes, D., Sivakumar, V., Glynn, D., Clarke, G. 2007. A case study: delayed failure of a deep cutting in lodgement till. *Geotechnical Engineering* 160 (GE4), 193-202.

Kim, T.H., and Hwang, C. 2003. Modelling of tensile strength on moist granular earth material at low water content. *Engineering Geology*, 69: 233-244.

Konrad, J-M. & Ayad, R. 1997. Desiccation of a sensitive clay: field experimental observations. *Can Geotech J*, 34, No. 6, 929–42.

Lakshmikantha, M.R., Prat, P.C. & Ledesma, A. 2012. Experimental evidence of size effect in soil cracking. *Canadian Geotechnical Journal*, 49, No. 3, 264-284.

Marsland, A. 1968. The shrinkage and fissuring of clay in flood banks. Building Research Station, Internal report No. 39/68.

Marsland, A. & Cooling, L.F. 1958. Tests on Full Scale Clay Flood Bank to Study Seepage and the Effects of Overtopping. Building Research Station, Internal report No. C562.

Morris, PH., Graham, J. & Williams, DJ. 1992. Cracking in drying soil. *Can Geotech*, 29, 263–77.

Péron H., Hu, L., Laloui, L. & Hueckel, T. 2007. Numerical and Experimental investigation of desiccation of soil;3:3–8.

Péron, H., Delenne, J.Y., Laloui, L. & El Youssoufi, M.S. 2009. Discrete element modelling of drying shrinkage and cracking of soils. *Comput Geotech*, 36, (1–2), 61–69.

Péron H, Hueckel T, Laloui L, Hu L. 2009. Fundamentals of desiccation cracking of fine-grained soils: experimental characterisation and mechanisms identification. *Can Geotech J*, 46:1177–201.

Prat, P.C., Ledesma, A., Lakshmikantha, M.R., Levatti, H.U., & Tapia, J. 2008. Fracture mechanics for crack propagation in drying soils. 12th International Conference of IACMAG, pp.106-1067.

Rodriguez, R.L. 2002. Estudio experimenntal de flujo y transporte de cromo, niquel y manganeso en resduos de la zona minera de Moa (Cuba): influencia del comportamiento hidromecanico. Ph.D. thesis, Universitat Politecnica de Catalunya – Barcelona Tech, Barcelona, Spain.

Rodriguez, R., Sanchez, M., Ledesma, A. & Lloret, A. 2007. Experimental and numerical analysis of desiccation of a mining waste. *Can Geotech J*, 44, No. 6. 644–658.

Sánchez, M., Manzoli, O.L. & Guimarães, L.J.N. 2014. Modeling 3-D desiccation soil crack networks using a mesh fragmentation technique. *Comput Geotech*, 62, 27–39.

Sherard, J.L. 1986. Hydraulic Fracturing in Embankment Dams. *Journal of Geotechnical Engineering,* 112 (10), 905-927.

Shin, H. & Santamarina, JC. 2011. Desiccation cracks in saturated fine-grained soils: particle-level phenomena and effective-stress analysis. *Géotechnique,* 61, No. 11, 961–72.

Sima, J., Jiang, M. & Zhou, C. 2014. Numerical simulation of desiccation cracking in a thin clay layer using 3D discrete element modeling. *Comput Geotech*, 56, 168–80.

Stirling, R. A., Hughes, P. N., Davie, C. T. & Glendinning, S. 2015. Tensile behaviour of unsaturated compacted clay soils — A direct assessment method. *Applied Clay Science* 112-113: 123-133.

Tang, G. X., and Graham, J. 2000. "A method for testing tensile strength in unsaturated soils. *Geotech. Testing J*., 23(3), 377–381.

Tang C-S, Pei X-J, Wang D-Y, Shi B, and Li J 2015. Tensile Strength of Compacted Clayey Soil. *J. Geotech. Geoenviron. Eng.* 141(4).

Tarantino, A. & Mongiovì, L. 2002. Design and construction of a tensiometer for direct measurement of matric suction. *Proceedings 3rd International Conference on Unsaturated Soils*. vol. 1. pp. 319-324. Edited by J.F.T. Jucá, T.M.P. de Campos and F.A.M. Marinho, Balkema, Rotterdam.

Tarantino, A. 2007. A possible critical state framework for unsaturated compacted soils. *Geotechnique,* 57, No. 4, 385-389.

Tarantino, A. 2009. A water retention model for deformable soils, *Géotechnique*, 59, No. 9, 751-762.

Tarantino, A., Sacchet, A., Dal Maschio, R. & Francescon, F. 2010. A Hydromechanical Approach to Model Shrinkage of Air-Dried Green Bodies. *Journal of the American Ceramic Society*, 93, No. 3, 662–670.

Tarantino, A. & El Mountassir, G. 2013. Making unsaturated soil mechanics accessible for engineers: preliminary hydraulic-mechanical characterisation and stability assessment. *Engineering Geology*, 165, 89-104.

Thusyanthan, N.I., Take, W.A., Madabhushi, S.P.G. & Bolton, M.D. 2007. Crack initiation in clay observed in beam bending. *Geotechnique,* 57, No. 7, 581–594

Trabelsi, H., Jamei, M., Zenzri, H., Olivella, S., 2012. Crack patterns in clayey soils: experiments and modeling. *Int. J. Numer. Anal. Methods Geomech*. 36, 1410–1433.

Vanapalli, S.K., Fredlund, D.G., Pufahl, D.E. & Clifton, A.W. 1996. Model for the prediction of shear strength with respect to soil suction. Canadian Geotechnical Journal, 33, No. 3, 379–392.

Varsei, M., Miller, G.A. & Hassanikhah, A., 2016. Novel Approach to Measuring Tensile Strength of Compacted Clayey Soil during Desiccation. International Journal of Geomechanics, 16 (6): D4016011.

Villar, L.F.S., de Campos, T.M.P., Azevedo, R.F., and Zornberg, J.G. 2009. Tensile Strength Changes under Drying and its Correlations with Total and Matric Suctions. Proceedings of the Seventeenth International Conference of Soil Mechanics and Geotechnical Engineering, Alexandria, Egypt, 5-9 October, pp. 793-796.

Yesiller N, Miller CJ, Inci G, Yaldo K. 2000. Desiccation and cracking behavior of three compacted landfill liner soils. *Eng Geol,* 57:105–21.

11. LIST OF CAPTIONS FOR TABLES

Table 1 Initial conditions for uniaxial compression and triaxial compression tests

12. LIST OF CAPTIONS FOR ILLUSTRATIONS

Figure 1 Uniaxial tension and compression specimen shape and dimensions (mm)

Figure 2 Apparatus for uniaxial tension test

Figure 3 Apparatus for uniaxial compression test

Figure 4 VC material (a) relationship between gravimetric moisture content and degree of saturation (b) relationship between gravimetric moisture content and suction

Figure 5 SK material (a) relationship between gravimetric water content and degree of suction (b) relationship between gravimetric moisture content and suction

Figure 6 Comparison of uniaxial tension tests performed at different loading rates on VC samples. (a) Shear strength envelope in the plane isotropic effective stress p' versus deviator stress q (b) Evolution of pore-water pressure during shearing for two specimens with similar initial pore water pressures tested at different loading rates

Figure 7. Evolution of pore-water pressure measured by the HCTs during the uniaxial compression test on VC (w=19.7%).

Figure 8 Stress-paths and water contents at failure for uniaxial and triaxial compression tests for VC

Figure 9 Evolution of pore-water pressure measured by the HCTs during the uniaxial tension test on non-de-aired VC (Test 21-10).

Figure 10 Stress-paths and water contents at failure for uniaxial tension tests for non-de-aired VC

Figure 11 Stress-paths and water contents at failure for uniaxial and triaxial compression tests for SK

Figure 12 Stress-paths and water contents at failure for uniaxial tension tests for non-de-aired SK

Figure 13 Stress-paths and water contents at failure for uniaxial tension tests for -de-aired VC

Figure 14 Stress-paths and water contents at failure for uniaxial tension tests for -de-aired SK

Figure 15 Theoretical angle between planes of failures and minor principal plane